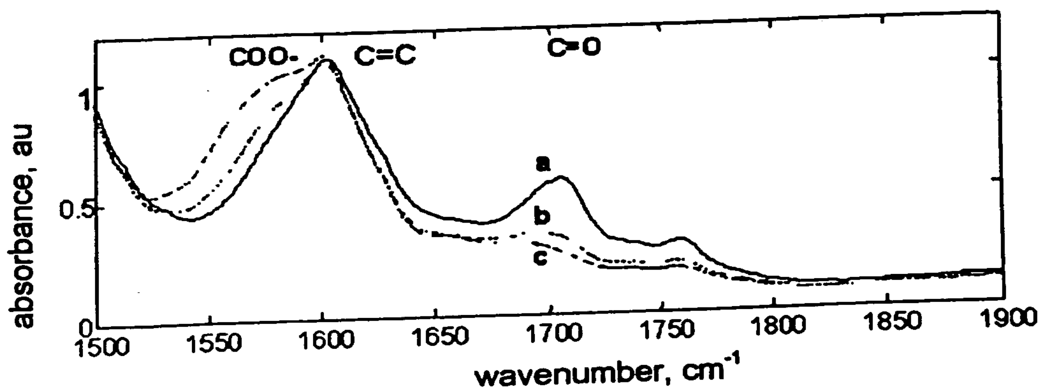

Fig. 1A. IR Absorbance Bands of C=O, Aromatic C=C, and Carboxylate COO- of a Distillate Residuum Fraction.

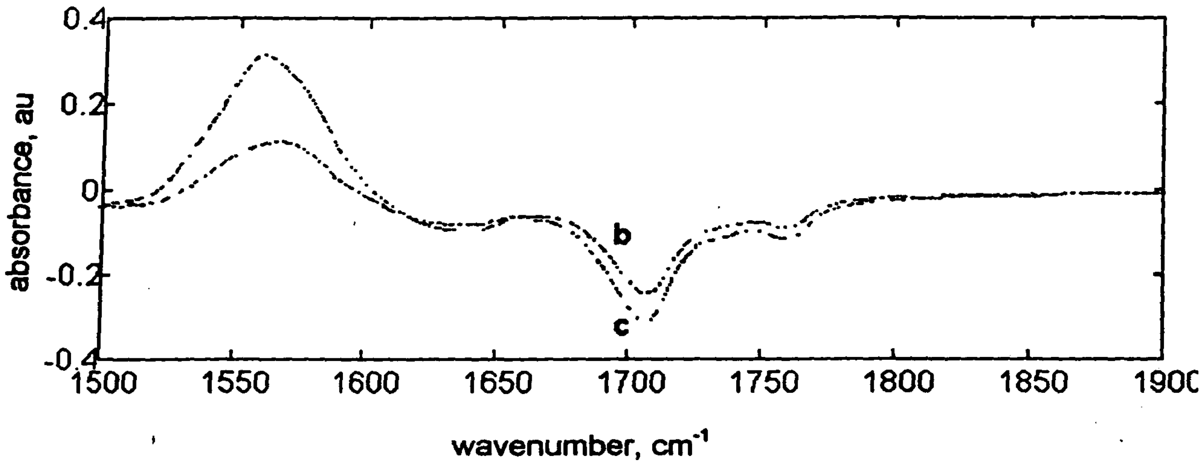

Fig. 1B. Absorbance Difference Between Treated Blends (curves b and c) and the Initially Untreated Blend of Distillate Residuum Fraction.

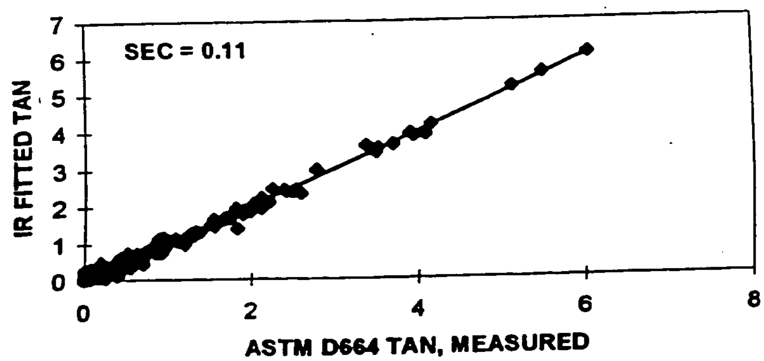

Fig. 2A. Fitted Values of IR TAN using the Calibration Model and Measured ASTM TAN for 216 Plant and Laboratory Distillation Samples.

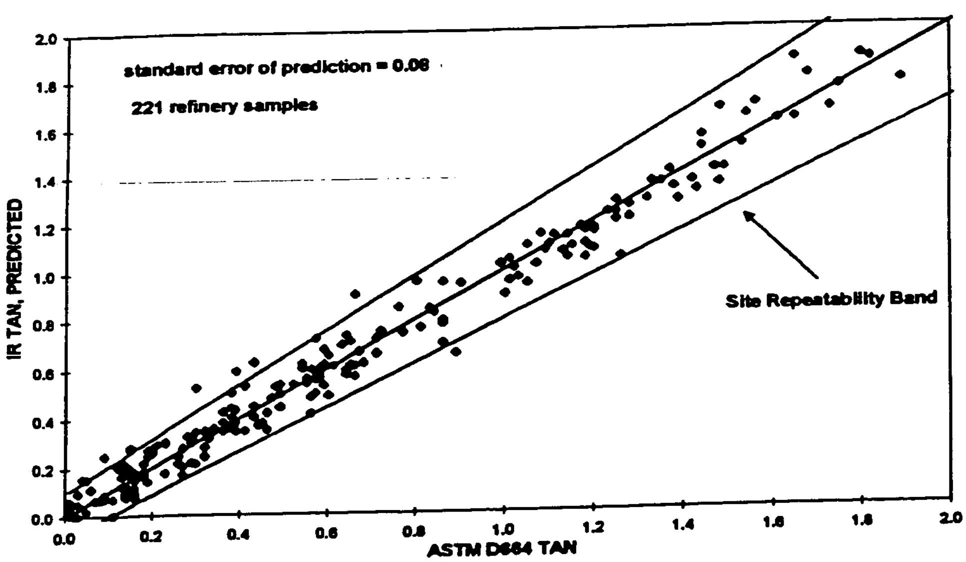

Fig. 2B. Predicted IR TAN and Measured ASTM TAN for 221 Refinery Samples.

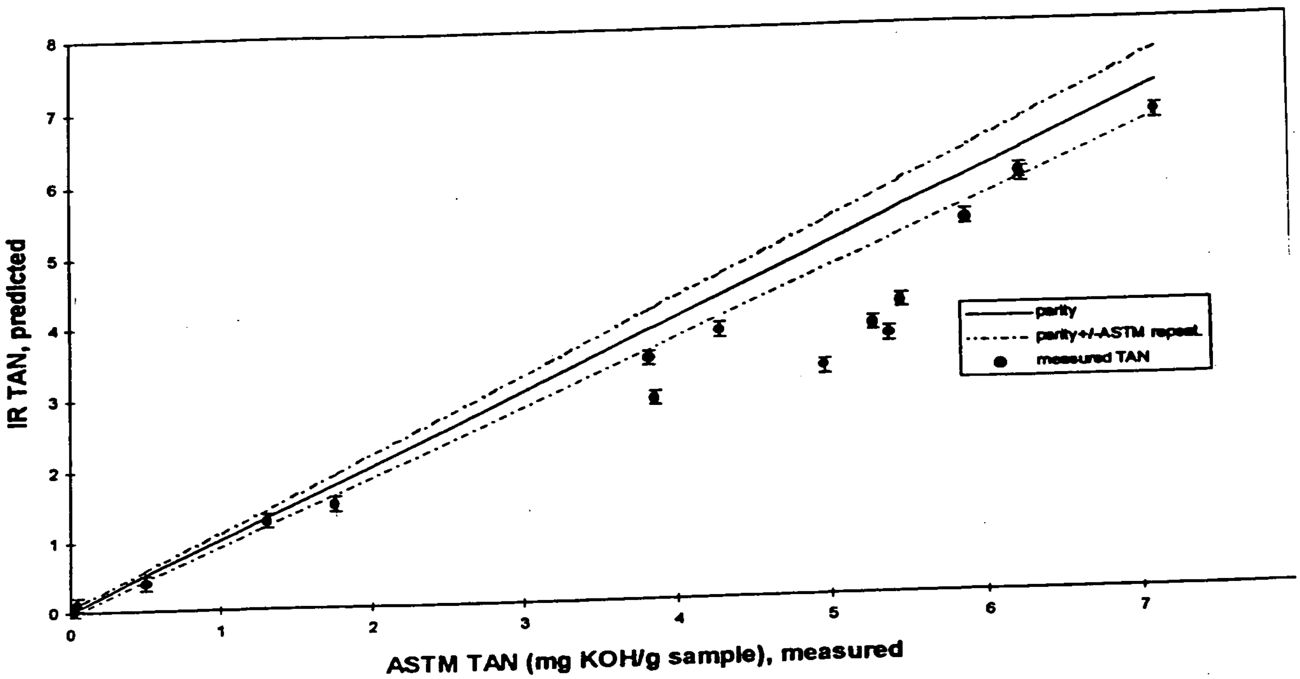

Fig. 3. IR TAN is Significantly Less than ASTM TAN for Samples with High Levels of Calcium Naphthanate.

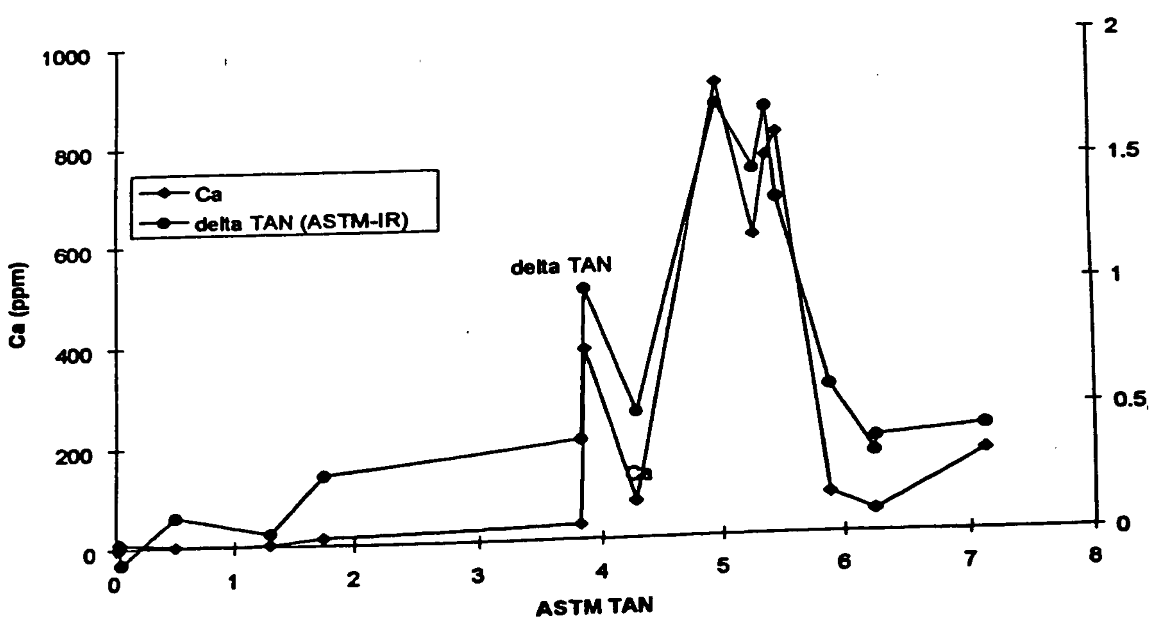

Fig. 4. Large Differences between IR and ASTM TAN Coincides with High Calcium Levels.

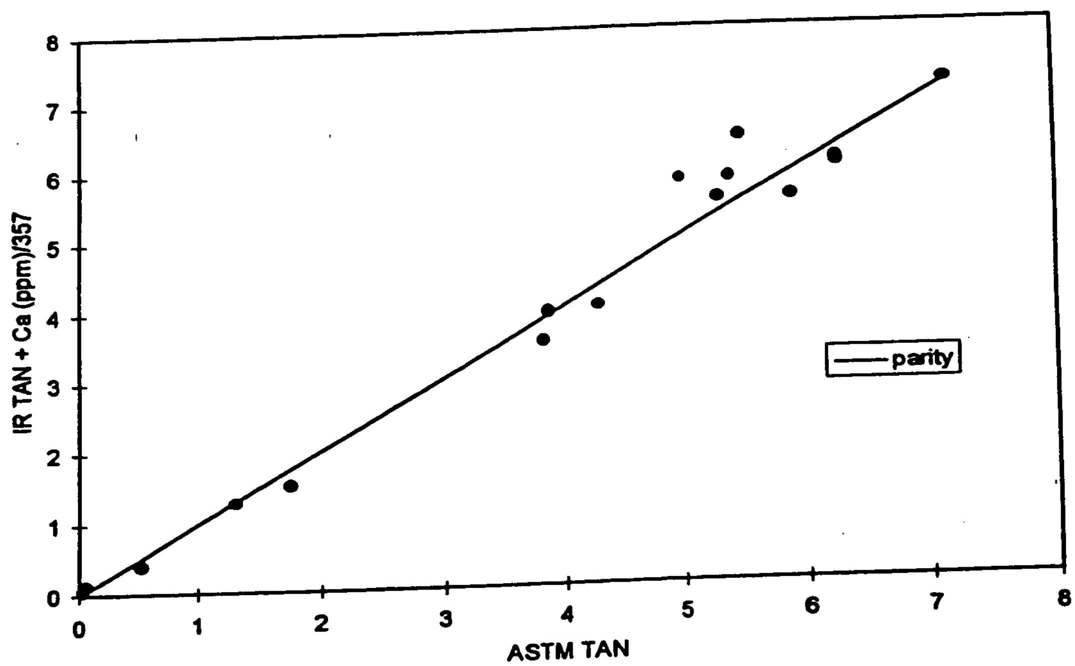

Fig. 5. Calcium Accounts for Difference between IR and ASTM TAN.

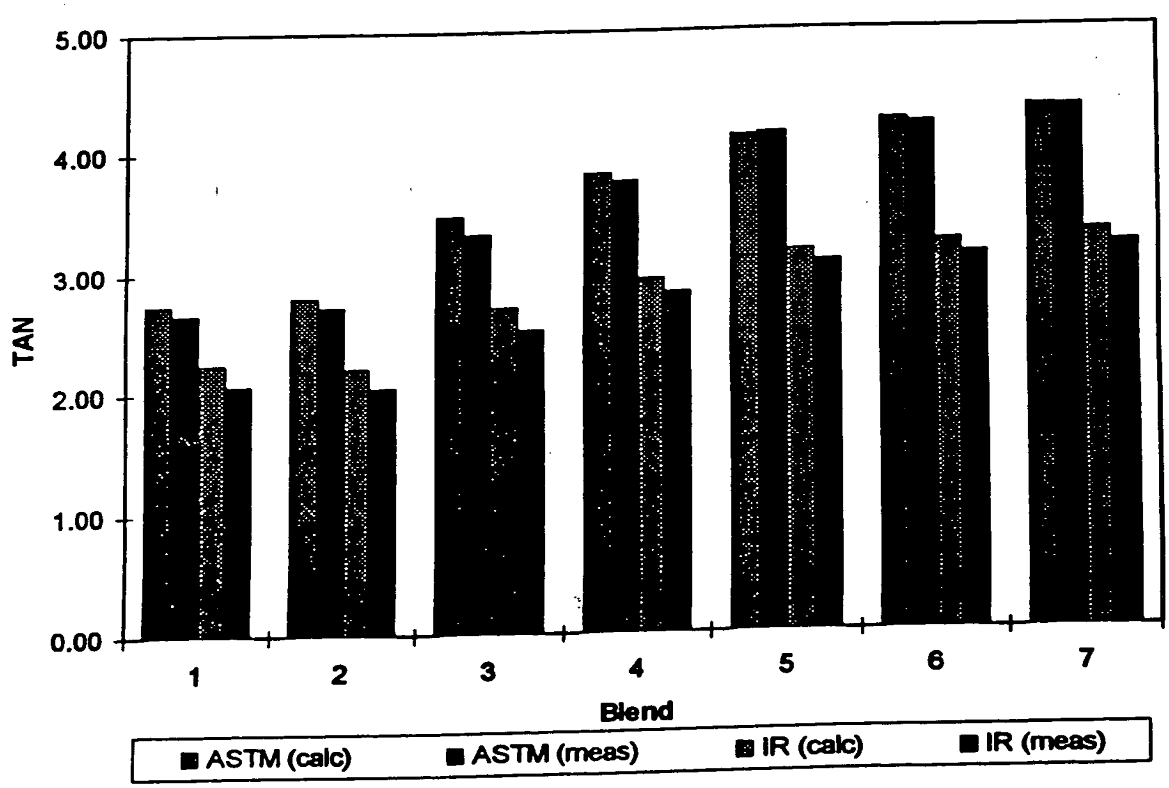

Fig. 6. IR TAN Blends Linearly and is Less than ASTM TAN for B, M, K Crude Blends.

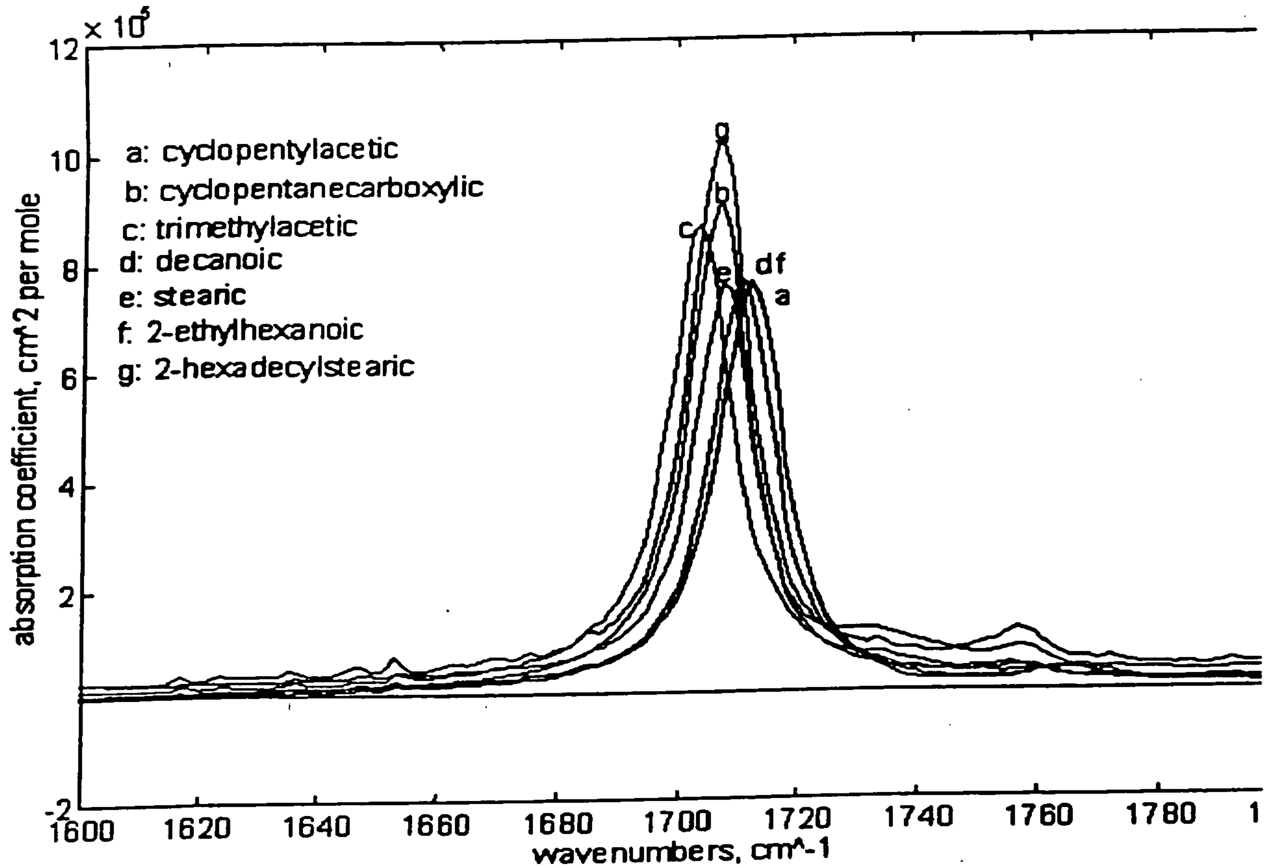

Fig. 7. Absorption Cross-Section of Model Acids Vary in Strength and Spectral Frequency.

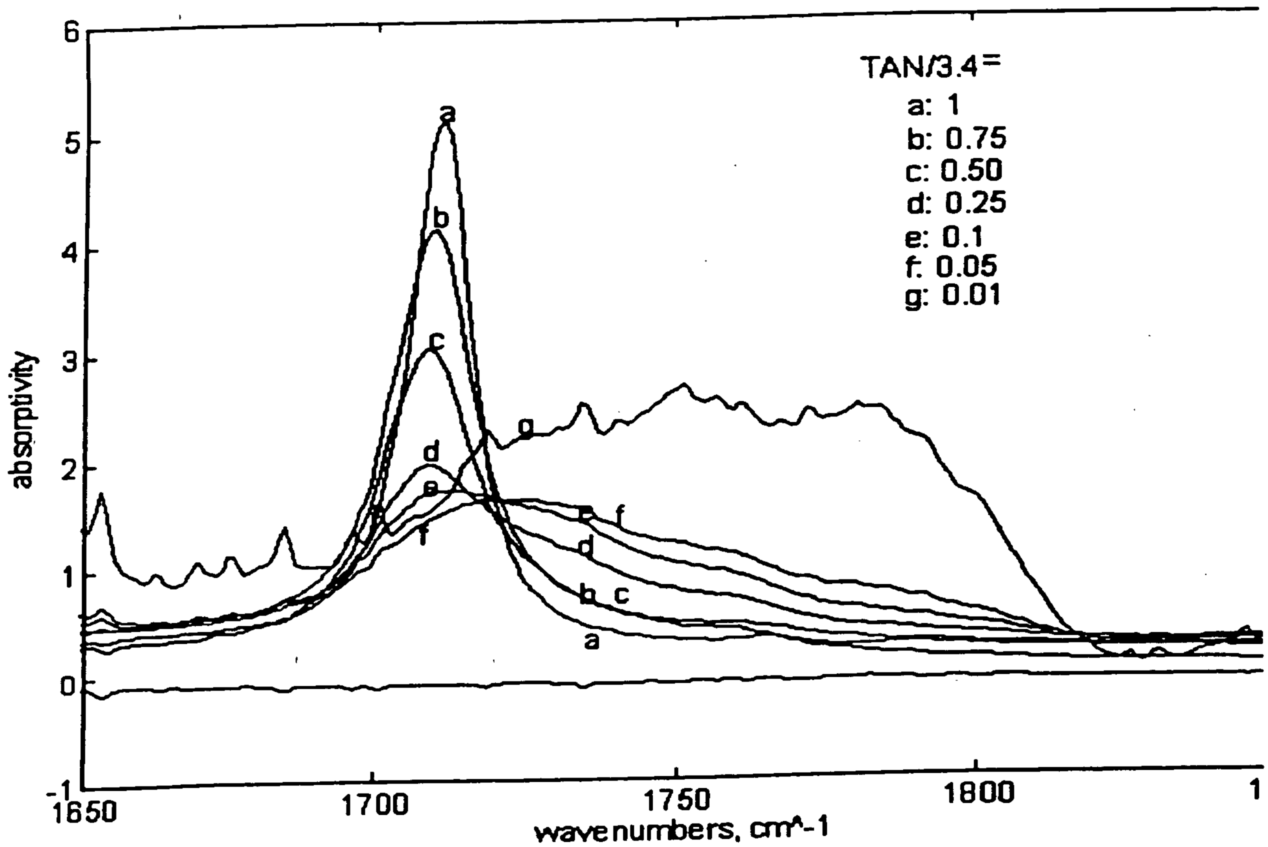

Fig. 8. Change in Shape of C=O Absorption Band with Concentration Due to Solvent Interactions.

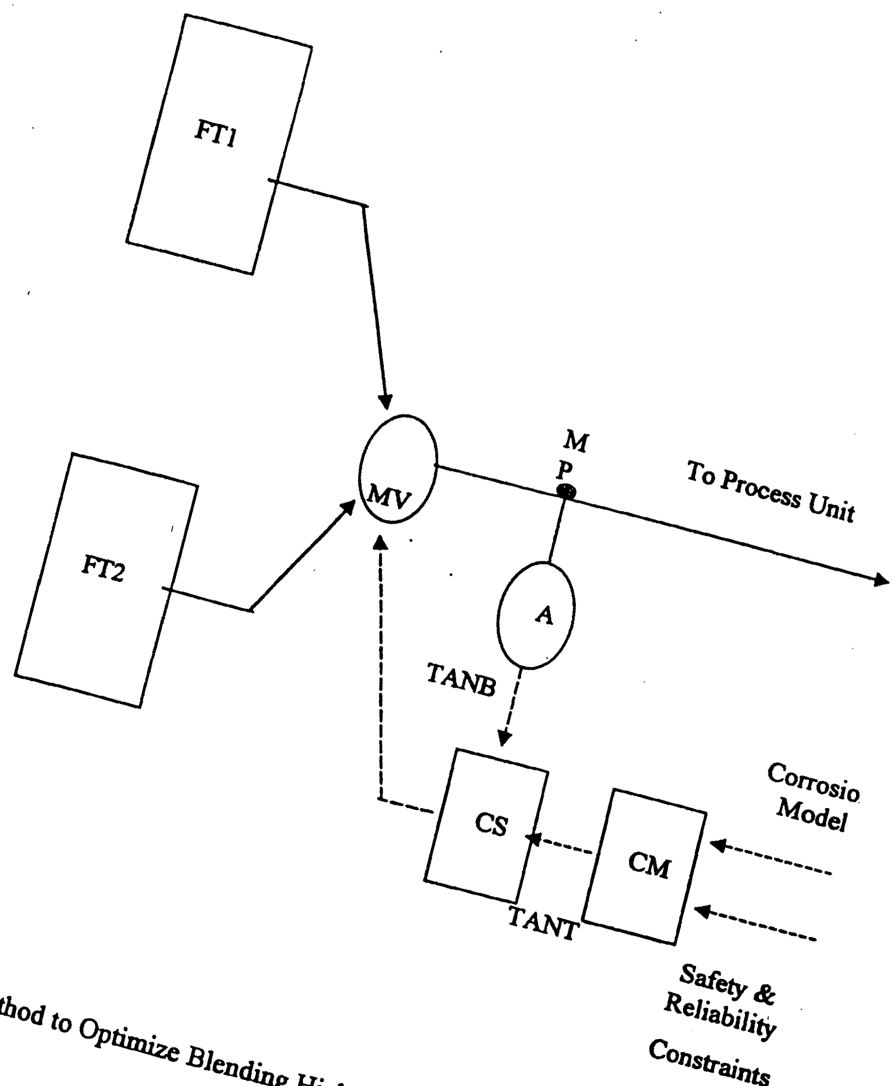

Fig. 9. Method to Optimize Blending High and Low TAN Feeds.

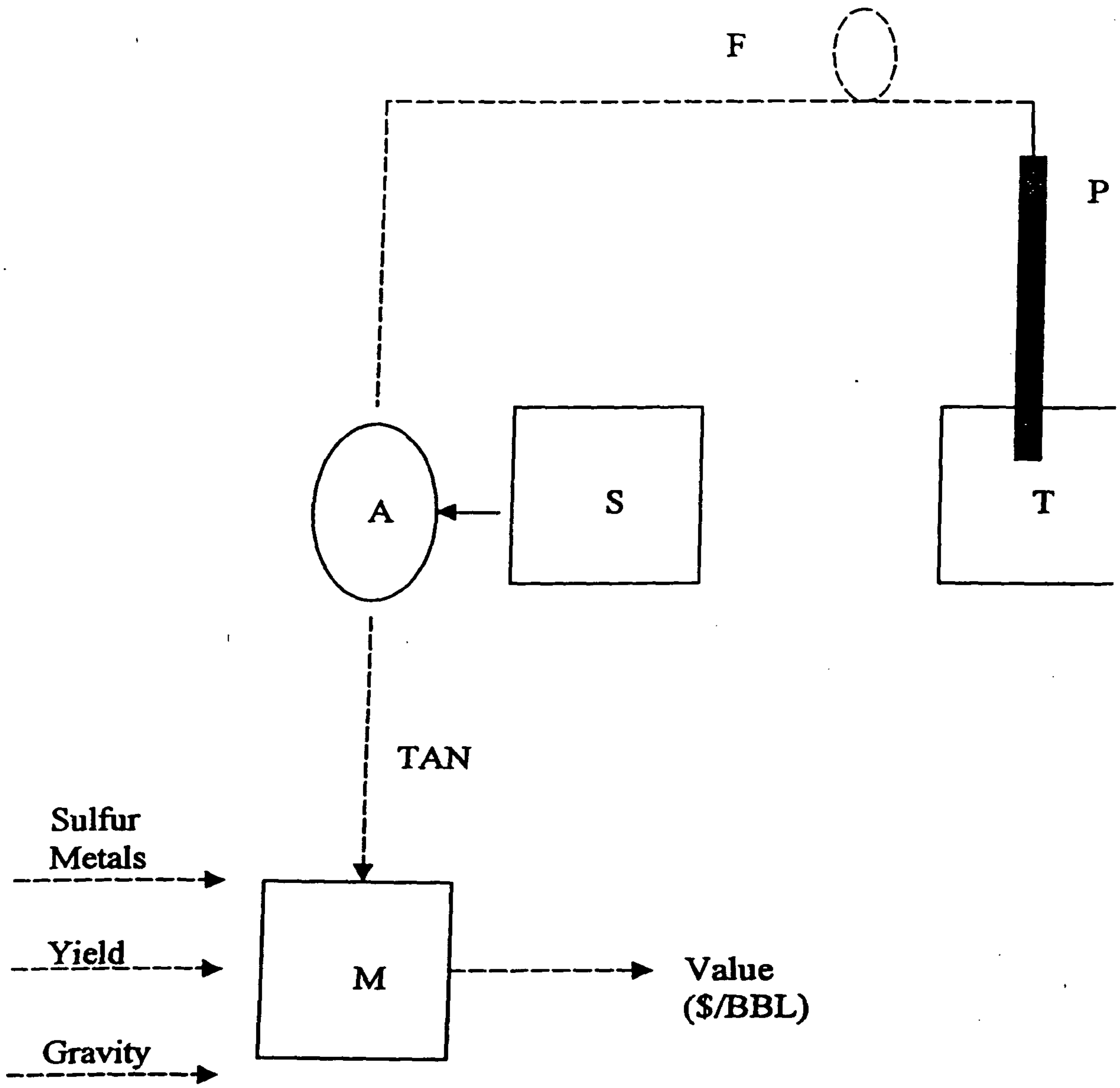

Fig. 10. Method to Optimize Valuation of Corrosive Crudes.

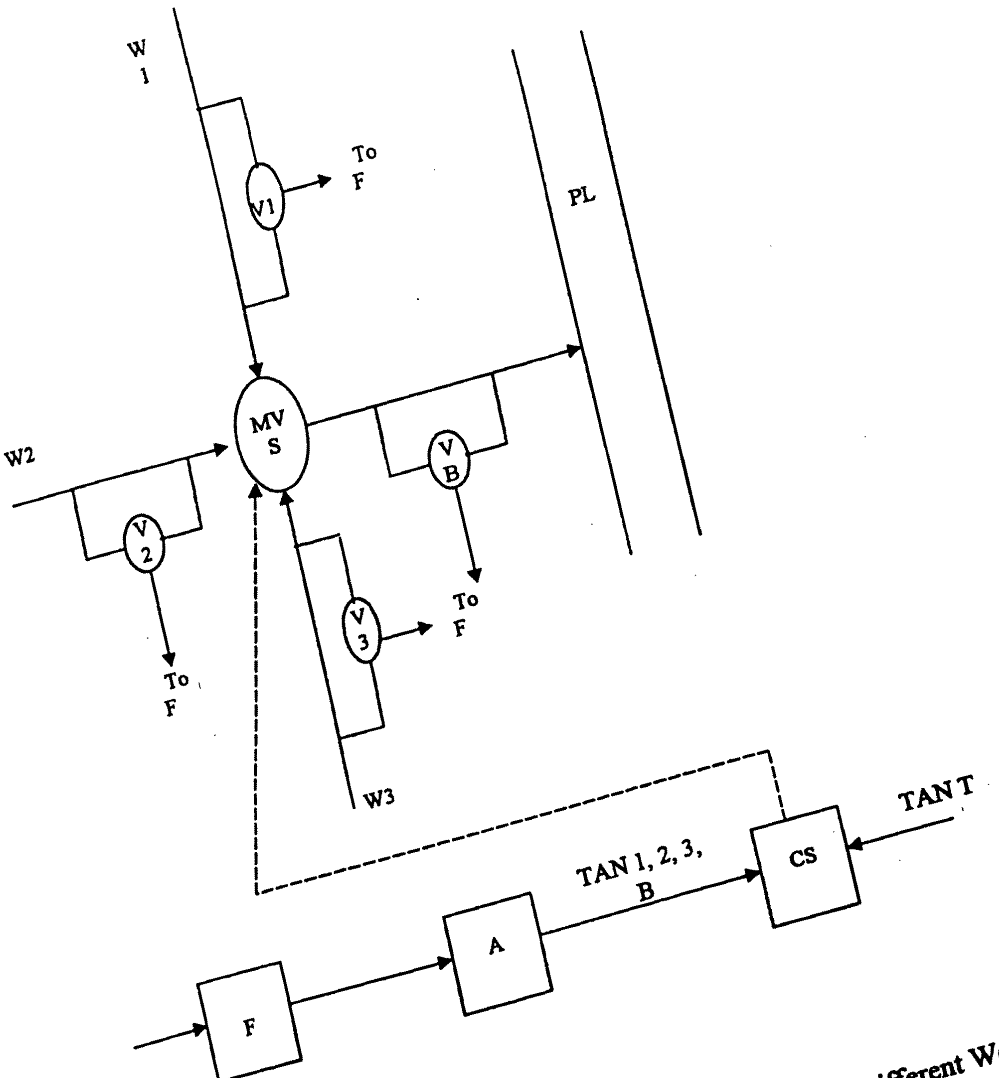

Fig. 11. Method to Optimize the Blending of Crude Oils from Different Wells a Target TAN for Pipeline Shipment.

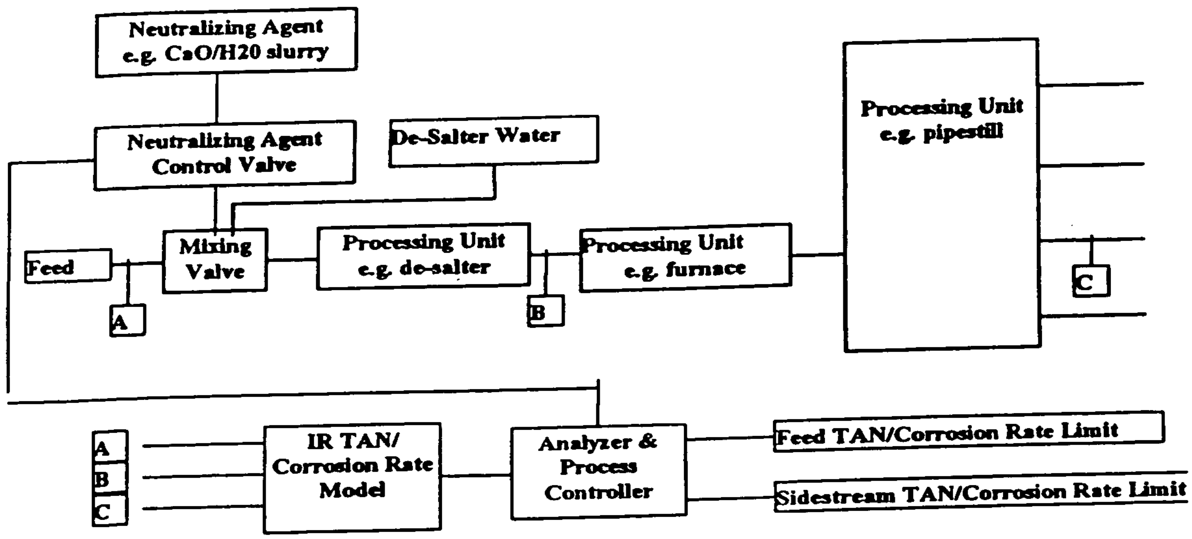

Fig. 12. Method to Optimize TAN Neutralization Process.